

High Harmonic Spectroscopy of the Cooper Minimum in Molecules

M. C. H. Wong,¹ A.-T. Le,² A. F. Alharbi,¹ A. E. Boguslavskiy,¹ R. R. Lucchese,³ J.-P. Brichta,¹
C. D. Lin,² and V. R. Bhardwaj^{1,*}

¹*Department of Physics, University of Ottawa, 150 Louis-Pasteur, Ottawa, Ontario K1N 6N5, Canada*

²*J. R. Macdonald Laboratory, Kansas State University, Manhattan, Kansas 66506-2604, USA*

³*Department of Chemistry, Texas A&M University, College Station, Texas 77843-3255, USA*

(Received 8 June 2012; published 18 January 2013)

The Cooper minimum (CM) has been studied using high harmonic generation solely in atoms. Here, we present detailed experimental and theoretical studies on the CM in molecules probed by high harmonic generation using a range of near-infrared light pulses from $\lambda = 1.3$ to $1.8 \mu\text{m}$. We demonstrate the CM to occur in CS_2 and CCl_4 at ~ 42 and ~ 40 eV, respectively, by comparing the high harmonic spectra with the known partial photoionization cross sections of different molecular orbitals, confirmed by theoretical calculations of harmonic spectra. We use CM to probe electron localization in Cl-containing molecules (CCl_4 , CH_2Cl_2 , and *trans*- $\text{C}_2\text{H}_2\text{Cl}_2$) and show that the position of the minimum is influenced by the molecular environment.

DOI: [10.1103/PhysRevLett.110.033006](https://doi.org/10.1103/PhysRevLett.110.033006)

PACS numbers: 33.20.Lg, 42.65.Ky

The electronic structure of atoms and molecules is mainly studied using photoelectron spectroscopy. Photoionization cross sections (PICS) and angular distribution parameters, determined as a function of photon energy, enable us to probe the nature of atomic and molecular orbitals. In atoms, if an orbital has a radial node, the dipole matrix element describing the transition from initial ground state to final continuum state can change sign as a function of photon energy. The PICS undergoes a Cooper minimum (CM) at the photon energy coinciding with the sign change [1]. An analogous effect was also observed in the photoionization of molecules containing atoms that are known to exhibit a CM [2].

High harmonic generation (HHG), in which an electron removed by the incident laser field gains energy from the field and recombines with the parent ion emitting high-energy photons [3], can also be used to probe the structure and dynamics of the recombining system that is encoded in the emitted harmonic spectrum. HHG is a new spectroscopic probe with the potential for angstrom spatial and attosecond temporal resolution, set by the shortest de Broglie wavelength of the recolliding electron and by the subcycle recollision dynamics, respectively. It has been used to image molecular orbitals [4], electronic wave packets [5], and nuclear dynamics [6] in simple aligned molecules as well as to probe collective multielectron dynamics [7] in atoms.

The recombination matrix element in the HHG process is, in essence, the inverse of photoionization, and the CM results in an amplitude modulation of the harmonic spectrum that is independent of both laser wavelength and intensity. To date, high harmonic spectroscopy has only been used to study CMs associated with the electronic structure of noble gases such as Ar [8,9] and Kr [7]. Several recent experimental and numerical studies [10–12]

have focused on the origin of a shift in the position of the CM between photoionization and HHG emission. Whereas high harmonic spectroscopy has been successful in probing atomic and some simple molecular systems, extending this tool to polyatomic molecules has been difficult due to the complex nature of molecular orbitals and multielectron dynamics, thus restricting its viability as a general spectroscopic tool. Since multicenter [13] and multiorbital interferences [14] can also modulate the harmonic spectrum along with the CM, disentangling these effects is challenging in molecules.

In this Letter, we show that HHG in randomly oriented molecules containing S and Cl atoms exhibits a CM. We present the first observation of a CM in the harmonic spectrum of CS_2 and show that it agrees very well with experimental PICS. Theoretical calculations of PICS and harmonic spectra in CS_2 confirm our results. To understand how the atomic nature of a particular molecular orbital influences the photoionization dynamics, we generated high harmonics in CCl_4 , CH_2Cl_2 , and *trans*- $\text{C}_2\text{H}_2\text{Cl}_2$. In these molecules, the CM was monitored over a range of wavelengths and intensities that allowed its identification.

High harmonics were produced in a finite gas cell of length 10 mm with 0.6 mm apertures. A 30 cm achromatic lens was used to focus 1.3–1.8 μm near-infrared (NIR) light pulses into the gas cell through a 2 mm thick calcium fluoride window. An optical parametric amplifier pumped by a Ti:sapphire regenerative amplifier (3.5 mJ, 40 fs, 100 Hz, 0.8 μm) produced 80 fs NIR pulses whose energies varied from 0.9 mJ at 1.8 μm to 1.3 mJ at 1.3 μm . The harmonics were dispersed by a flat-field concave grating at grazing incidence onto a microchannel plate detector coupled to a phosphor screen and then imaged by a charge-coupled device camera. The spectrometer was calibrated by measuring the transmitted spectrum after an

aluminum filter. Intensity calibration of the laser beam was achieved by monitoring the cutoff harmonics from HHG in Ar and validated by measuring its saturation intensity using a fast ionization gauge. The position of the laser focus in the gas cell was adjusted such that the highest yield of cutoff harmonics was produced, thereby favoring short trajectories. The vapor pressures of all liquids at room temperature were high enough for them to be introduced into the gas cell without need for a carrier gas. Each liquid underwent a freeze and thaw cycle to minimize contamination in the gas cell.

Since most molecules have ionization potentials (IP) in the range of 9–11 eV, longer wavelengths ($\lambda = 1.3\text{--}1.8\ \mu\text{m}$) (a) ensure adiabatic ionization, (b) extend the cutoff harmonics to beyond 50 eV which is needed to capture signatures of molecular and multielectron dynamics [15], and (c) favor phase matching at higher gas pressures, thereby partially offsetting the wavelength scaling of high harmonic signal [16].

Though CM is an atomic phenomenon, it persists in molecules containing atoms whose orbitals exhibit a radial node. We present experimental and theoretical studies on the CM in CS_2 (IP = 10.07 eV) and CCl_4 (IP = 11.47 eV) using high harmonic spectroscopy and extend it to other Cl-containing complex molecules. The top panels of Fig. 1 show experimental high harmonic spectra of CS_2 [Fig. 1(a)] and CCl_4 [Fig. 1(b)] obtained with $1.8\ \mu\text{m}$ light at an intensity of $\sim 9 \times 10^{13}\ \text{W}/\text{cm}^2$. For comparison, we also show the published PICS for lone-pair orbitals of CS_2 ($2\pi_g$) [17] and CCl_4 ($2t_1$) [2] obtained by angle-resolved photoelectron spectroscopy. Since lone-pair orbitals can be

associated with a particular nucleus or atom, the observed minimum in the experimental PICS of these orbitals is analogous to photoionization of the $3p$ orbital of S and Cl atoms, which are known to exhibit CM at ~ 42 [18] and ~ 43.5 eV [19], respectively.

The observed local minimum in the harmonic spectrum of CS_2 at ~ 42 eV [Fig. 1(a)] coincides well with the minimum in the PICS. The relative harmonic amplitudes are in good agreement with the known PICS in the energy range of $\sim 30\text{--}60$ eV. They differ at high energies due to a sudden drop in the harmonic signal in the cutoff region and at low energies due to poor phase matching as well as reabsorption of generated harmonics, which is typical for a gas cell. Similarly, the $2t_1$ orbital of CCl_4 also displays a minimum near ~ 43 eV [2], which is in fairly good agreement with the harmonic spectrum where the minimum is at ~ 40 eV [Fig. 1(b)].

The bottom panels of Fig. 1 show theoretical PICS as well as calculated high harmonic spectra for both CS_2 [Fig. 1(c)] and CCl_4 [Fig. 1(d)] obtained using $1.8\ \mu\text{m}$ light at an intensity of $\sim 6 \times 10^{13}\ \text{W}/\text{cm}^2$. Calculations for cross sections were obtained using EPOLYSCAT [20,21]. Theoretical high harmonic spectra for these molecules were obtained within a single-molecule response approximation using the quantitative rescattering (QRS) theory [22] with the transition dipole calculated from EPOLYSCAT and the ionization rate calculated within the strong-field approximation.

Local minima appear in both calculated PICS and high harmonic spectra for both molecules. In CS_2 , this minimum appears at ~ 49 eV, which is 7 eV higher than the observed position of the minimum from experiment. The discrepancy in the position of the minimum in the high harmonic spectra can be attributed to the differences between the theoretical and experimental PICS. To avoid confusion, we note that these PICS are averaged over the isotropic molecular distribution, whereas according to the QRS, the complex valued transition dipole for a fixed-in-space molecule is used for HHG simulation. The angular averaging is carried out coherently after the induced dipole is obtained. Therefore, the position of the CM in angular-averaged PICS and that of the corresponding high harmonic spectrum could be somewhat different. In this respect, it should be of great interest to measure the CM position in HHG spectra with aligned molecules. In CCl_4 , the minimum in both experimental and calculated harmonic spectra appears at ~ 40 eV. However, the minimum in theoretical PICS is shifted to higher photon energy (~ 48 eV) compared to that of experiments. Despite these differences, the calculations confirm the existence of a CM in molecules and fairly reproduce the relative shape of the harmonic spectra. We expect that macroscopic propagation and ground state depletion reduce the theoretical harmonic yield near the cutoff, thus bringing it to a better agreement with experiment.

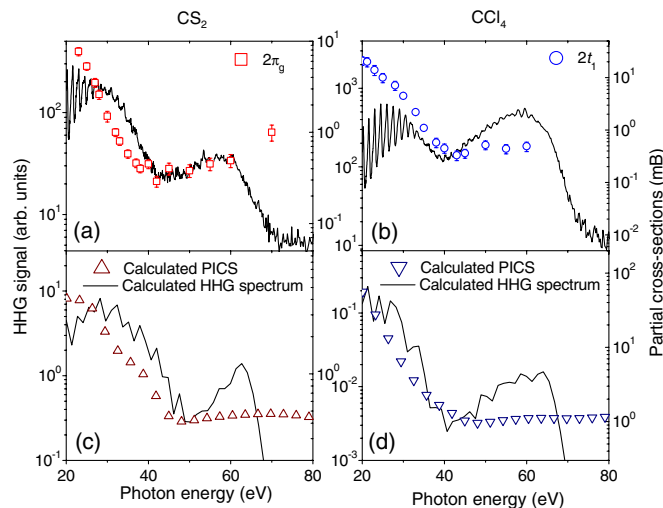


FIG. 1 (color online). Top (bottom) panels are experimental (theoretical) HHG spectra using $\lambda = 1.8\ \mu\text{m}$ wavelength light with intensity $\sim 9 \times 10^{13}\ \text{W}/\text{cm}^2$ ($\sim 6 \times 10^{13}\ \text{W}/\text{cm}^2$) along with experimental and theoretical (open symbols) partial PICS for (a) CS_2 and (b) CCl_4 . Only the envelopes are shown in theoretical HHG spectra.

The degree of atomic character in molecular orbitals influences the position of the CM, which can vary for either (a) different orbitals of a given molecule or (b) different molecular environments. Thus, the CM can be used to probe the atomic nature of molecular orbitals. To enable this, it is imperative to clearly identify the position of the CM in high harmonic spectra. However, recent studies have shown that even in simple systems such as in Ar discrepancies in the position of CM exist between different measurements and between theory and experiment.

HHG experiments carried out at 0.8, 1.2, and 2 μm have determined the CM in Ar to lie between 50 and 54 eV [8,11,12] whereas single photon measurements [23] and theoretical calculations [24] of PICS indicate the CM to occur at ~ 48 eV. According to the QRS theory, the CM in HHG is directly related to the CM in the differential PICS, which is slightly shifted with respect to the CM at 48 eV in the total (integrated) PICS. Moreover, the position of the CM in the HHG spectrum is influenced by the shape of the returning electron wave packet, which depends on the laser parameters and phase matching conditions. Indeed, the CM was shown to critically depend on phase matching conditions [10,12]. To understand this better, we extend the study of the CM in Ar by using a range of NIR driving wavelengths and intensities to generate high harmonics.

Figure 2 shows the measured position of the minimum in Ar using $\lambda = 1.3\text{--}1.8$ μm light as a function of intensity. The position of the minimum was extracted from each harmonic spectrum after smoothing. The use of long wavelengths reduces measurement uncertainty in determining the position of amplitude modulations since the harmonic comb spacing reduces with increasing wavelength. The error bar associated with each data point is equivalent to the energy of one harmonic order on either side of the minimum. Since phase matching was shown to be critical [10], we studied the position of the minimum for each wavelength at different pressures in the gas cell.

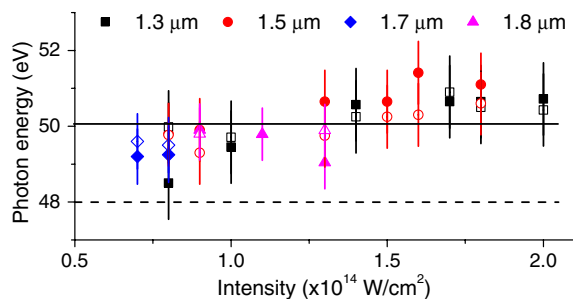


FIG. 2 (color online). Position of the Cooper minimum in HHG spectra for Ar as a function of intensity for different wavelengths $\lambda = 1.3\text{--}1.8$ μm . At each wavelength, we show the position for two different pressures (closed shapes, 45 Torr; open shapes, 25 Torr) in the finite gas cell. The dotted line at 48 eV corresponds to the position of the minimum in the experimental and theoretical PICS [23,24].

Our measurements show the position of the CM to be 50.1 ± 0.7 eV, independent of intensity, wavelength, and pressure in the gas cell (see Fig. 2). We observe a slight downshift of the minimum (49.4 eV) at lower intensities. This could be because at low intensities, the cutoff moves closer to the CM, thus influencing its position. This value for the position of the CM is in good agreement with theoretical simulations based on the QRS theory at the single-atom level [22] and with the inclusion of macroscopic propagation [11], where a single active-electron model potential suggested by Muller [25] was used. Calculation of the recombination transition dipole using field-free continuum wave functions within the same model potential approach also predicts the CM to occur near 51 eV [8,12,22].

We now return to the discussion on CM in molecules. The position of the CM might differ for different orbitals of a given molecule. In fact, calculations of PICS for the 2π and 5σ bands in HCl [26] indicate a variation of the CM position by a few eV. However, this would be difficult to study using high harmonic spectroscopy due to the lack of selectivity of a specific orbital. Here, we study the case where the CM can be affected by the molecular environment and therefore can vary for different molecules even when their molecular orbitals originate from the same atomic subshell (for example, the 3π orbital of Cl).

Figure 3(a) shows the harmonic spectra of three Cl-containing molecules using $\lambda = 1.8$ μm light with intensity $\sim 9 \times 10^{13}$ W/cm². Each harmonic spectrum exhibits a deep local minimum at 40.4 ± 0.5 eV (CCl_4 , IP = 11.47 eV), 42.1 ± 0.4 eV (CH_2Cl_2 , IP = 11.32 eV), and 43.2 ± 0.4 eV (*trans*- $\text{C}_2\text{H}_2\text{Cl}_2$, IP = 9.64 eV). The dashed line indicates the noted shift of the minimum between different molecules. We performed a systematic study to accurately determine the position of the minimum and whether it is influenced by the experimental conditions. Figures 3(b)–3(d) show the intensity dependence of the minimum in all molecules for different wavelengths whereas Fig. 3(e) shows the pressure dependence using $\lambda = 1.8$ μm light for CCl_4 and CH_2Cl_2 . The dotted lines indicate the average value of the position of the minimum for each molecule. The positions of the minima and the error bars were derived in the same fashion as that for Fig. 2.

The positions of the amplitude minima in the harmonic spectra for all three molecules are independent of laser intensity and gas pressure, which suggests that they arise due to CM. This interpretation is also confirmed from the theoretical calculations. Minima arising through dynamical interference from multiorbital contributions to ionization [14] depend strongly on the laser parameters (intensity and wavelength) and can therefore be excluded. In addition, any minima arising from structural interference due to multicenter recombination [13,27,28] in unaligned molecules are expected to be very weak. A local minimum is

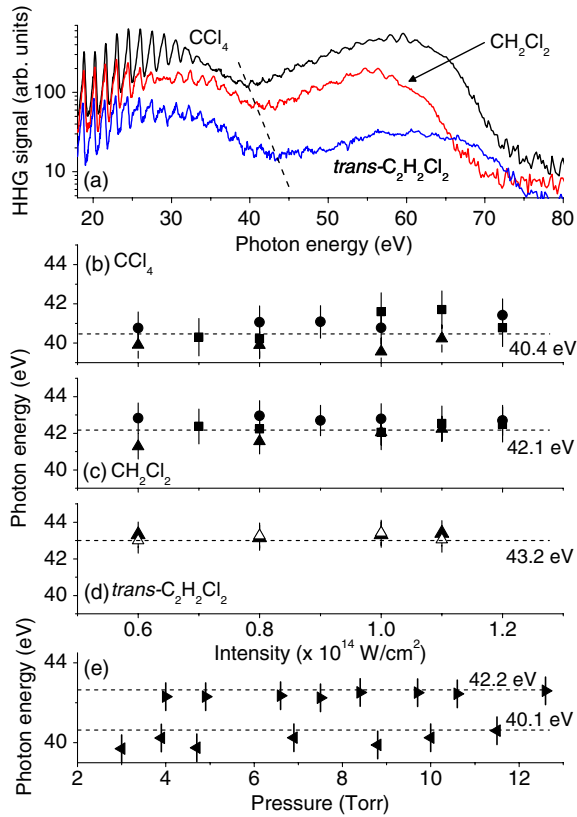


FIG. 3 (color online). (a) Harmonic spectra generated in CCl_4 , CH_2Cl_2 , and $\text{trans-C}_2\text{H}_2\text{Cl}_2$ using $\lambda = 1.8 \mu\text{m}$ and intensity $\sim 9 \times 10^{13} \text{ W/cm}^2$. The dashed line emphasizes the shift of the minimum between different molecules. [(b)–(d)] Position of minimum in harmonic spectra as a function of intensity for (b) CCl_4 and (c) CH_2Cl_2 with $P = 10 \text{ Torr}$ and $\lambda = 1.3 \mu\text{m}$ (filled squares), $1.5 \mu\text{m}$ (filled circles), $1.8 \mu\text{m}$ (filled triangles) as well as (d) $\text{trans-C}_2\text{H}_2\text{Cl}_2$ where $\lambda = 1.8 \mu\text{m}$ and $P = 10 \text{ Torr}$ (filled triangles), 3 Torr (hollow triangles). (e) Position of minimum as a function of pressure for CCl_4 (left hand side filled triangles) and CH_2Cl_2 (right hand side filled triangles) using $\lambda = 1.8 \mu\text{m}$ light with intensity $\sim 9 \times 10^{13} \text{ W/cm}^2$.

reported to be present in PICS measurements for at least one orbital in CH_2Cl_2 , but the position has not been published [29]. To our knowledge, PICS for $\text{trans-C}_2\text{H}_2\text{Cl}_2$ are not available for a direct comparison of the position of the CM, but the intensity-independent minimum in the harmonic spectrum is strong evidence that a CM must be present in the PICS.

The variation of CM in the three molecules is then a measure of the extent to which molecular orbitals retain part of their atomic character. To quantify the degree to which the $3p$ subshell of Cl exerts its influence on the molecular orbitals, we compare Mulliken atomic populations on Cl for each molecule. We performed *ab initio* calculations of the molecular orbitals at Hartree-Fock level using GAMESS [30]. In Fig. 4(a), we show the binding energies as well as the Mulliken atomic populations on Cl for all low-lying molecular orbitals of the three

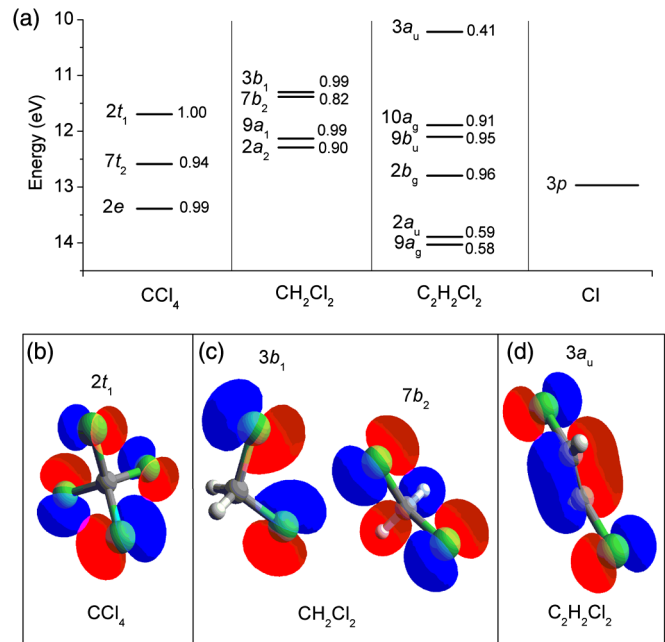


FIG. 4 (color online). (a) Binding energies and corresponding Mulliken atomic populations on Cl for molecular orbitals of CCl_4 , CH_2Cl_2 , and $\text{trans-C}_2\text{H}_2\text{Cl}_2$ as well as atomic Cl [2,33,34]. [(b)–(d)] Highest occupied molecular orbitals of (b) CCl_4 , (c) CH_2Cl_2 , and (d) $\text{trans-C}_2\text{H}_2\text{Cl}_2$.

molecules in addition to the $3p$ subshell of Cl. All molecular orbitals within the 11–14 eV range have lone-pair character and, consequently, have high Mulliken atomic populations on Cl. However, the highest occupied molecular orbital (HOMO) of $\text{trans-C}_2\text{H}_2\text{Cl}_2$ has bonding character from the C-Cl bond with some contribution from the $3p$ orbital of Cl [31]. Such bonding orbitals are also known to exhibit a minimum in their PICS known as a partial CM (for example, the $6a_1$ band in CCl_4 [2]).

The Mulliken atomic populations on Cl are 1.0, 0.9 [32], and 0.4 for the HOMOs of CCl_4 , CH_2Cl_2 , and $\text{trans-C}_2\text{H}_2\text{Cl}_2$, respectively. Thus, the influence of the $3p$ subshell of Cl is more significant in CCl_4 and less so in $\text{trans-C}_2\text{H}_2\text{Cl}_2$. This is apparent from the molecular orbitals shown in Fig. 4(b) and consistent with results from photoelectron spectroscopy where the visibility of the CM, represented by the depth in the angular distribution parameter, decreased as Cl atoms were replaced by H atoms in CCl_4 [29].

In conclusion, we demonstrate for the first time evidence of a CM in high harmonic spectra of unaligned polyatomic molecules. Experimentally, we show that CM can be a sensitive probe of the atomic nature of the molecular orbital since it is independent of laser parameters. From a theoretical point of view, CM can be used to test the validity of new tools that are being developed so that they can be extended to even complex molecules. The agreement between the experimental and theoretical HHG spectra suggests that in aligned molecules it is

possible to extract shapes of PICS for the HOMOs of molecules over a ~ 30 – 60 eV range using high harmonic spectroscopy, similar to the atomic case [7,9]. However, phase matching and dynamical interference from multi-orbital contributions to HHG would restrict extraction of cross sections over a large photon energy spectrum.

The authors gratefully acknowledge financial support from the Natural Science and Engineering Research Council of Canada, expert technical assistance from Bruno Schmidt and Antoine Laramée, and fruitful discussions with François Légaré and Thomas Brabec. A.-T.L., R.R.L., and C.D.L. are supported by the Chemical Sciences, Geosciences and Biosciences Division, Office of Basic Energy Sciences, Office of Science, U.S. Department of Energy.

*ravi.bhardwaj@uottawa.ca

- [1] J. W. Cooper, *Phys. Rev.* **128**, 681 (1962).
- [2] T. A. Carlson, M. O. Krause, F. A. Grimm, P. Keller, and J. W. Taylor, *J. Chem. Phys.* **77**, 5340 (1982).
- [3] P. B. Corkum, *Phys. Rev. Lett.* **71**, 1994 (1993).
- [4] J. Itatani, J. Levesque, D. Zeidler, H. Niikura, H. Pépin, J. C. Kieffer, P. B. Corkum, and D. M. Villeneuve, *Nature (London)* **432**, 867 (2004).
- [5] S. Haessler *et al.*, *Nat. Phys.* **6**, 200 (2010).
- [6] S. Baker, J. S. Robinson, C. A. Haworth, H. Teng, R. A. Smith, C. C. Chirilă, M. Lein, J. W. G. Tisch, and J. P. Marangos, *Science* **312**, 424 (2006).
- [7] A. D. Shiner, B. E. Schmidt, C. Trallero-Herrero, H. J. Wörner, S. Patchkovskii, P. B. Corkum, J.-C. Kieffer, F. Légaré, and D. M. Villeneuve, *Nat. Phys.* **7**, 464 (2011).
- [8] H. J. Wörner, H. Niikura, J. B. Bertrand, P. B. Corkum, and D. M. Villeneuve, *Phys. Rev. Lett.* **102**, 103901 (2009).
- [9] S. Minemoto, T. Umegaki, Y. Oguchi, T. Morishita, A.-T. Le, S. Watanabe, and H. Sakai, *Phys. Rev. A* **78**, 061402 (R) (2008).
- [10] J. P. Farrell, L. S. Spector, B. K. McFarland, P. H. Bucksbaum, M. Gühr, M. B. Gaarde, and K. J. Schafer, *Phys. Rev. A* **83**, 023420 (2011).
- [11] C. Jin, H. J. Wörner, V. Tosa, A.-T. Le, J. B. Bertrand, R. R. Lucchese, P. B. Corkum, D. M. Villeneuve, and C. D. Lin, *J. Phys. B* **44**, 095601 (2011).
- [12] J. Higué *et al.*, *Phys. Rev. A* **83**, 053401 (2011).
- [13] M. Lein, N. Hay, R. Velotta, J. P. Marangos, and P. L. Knight, *Phys. Rev. A* **66**, 023805 (2002).
- [14] O. Smirnova, Y. Mairesse, S. Patchkovskii, N. Dudovich, D. Villeneuve, P. Corkum, and M. Y. Ivanov, *Nature (London)* **460**, 972 (2009).
- [15] R. Torres *et al.*, *Opt. Express* **18**, 3174 (2010).
- [16] A. D. Shiner, C. Trallero-Herrero, N. Kajumba, H.-C. Bandulet, D. Comtois, F. Légaré, M. Giguère, J.-C. Kieffer, P. B. Corkum, and D. M. Villeneuve, *Phys. Rev. Lett.* **103**, 073902 (2009).
- [17] T. A. Carlson, M. O. Krause, and F. A. Grimm, *J. Chem. Phys.* **77**, 1701 (1982).
- [18] S. T. Manson, A. Msezane, A. F. Starace, and S. Shahabi, *Phys. Rev. A* **20**, 1005 (1979).
- [19] J. A. R. Samson, Y. Shefer, and G. C. Angel, *Phys. Rev. Lett.* **56**, 2020 (1986).
- [20] F. A. Gianturco, R. R. Lucchese, and N. Sanna, *J. Chem. Phys.* **100**, 6464 (1994).
- [21] A. P. P. Natalense and R. R. Lucchese, *J. Chem. Phys.* **111**, 5344 (1999).
- [22] A.-T. Le, R. R. Lucchese, S. Tonzani, T. Morishita, and C. D. Lin, *Phys. Rev. A* **80**, 013401 (2009).
- [23] J. A. R. Samson and W. C. Stolte, *J. Electron Spectrosc. Relat. Phenom.* **123**, 265 (2002).
- [24] W. Ong and S. T. Manson, *Phys. Rev. A* **21**, 842 (1980).
- [25] H. G. Muller, *Phys. Rev. A* **60**, 1341 (1999).
- [26] T. A. Carlson, M. O. Krause, A. Fahlman, P. R. Keller, J. W. Taylor, T. Whitley, and F. A. Grimm, *J. Chem. Phys.* **79**, 2157 (1983).
- [27] T. Kanai, S. Minemoto, and H. Sakai, *Nature (London)* **435**, 470 (2005).
- [28] M. C. H. Wong, J.-P. Brichta, and V. R. Bhardwaj, *Phys. Rev. A* **81**, 061402(R) (2010).
- [29] T. A. Carlson, M. O. Krause, W. A. Svensson, P. Gerard, F. A. Grimm, T. A. Whitley, and B. P. Pullen, *Z. Phys. D* **2**, 309 (1986).
- [30] M. W. Schmidt *et al.*, *J. Comput. Chem.* **14**, 1347 (1993).
- [31] L. Mei, M. Chuaqui, C. P. Mathers, J. F. Ying, and K. T. Leung, *Chem. Phys.* **188**, 347 (1994).
- [32] Average over close-lying HOMO ($3b_1$) and HOMO-1 ($7b_2$).
- [33] T. Pradeep and D. A. Shirley, *J. Electron Spectrosc. Relat. Phenom.* **66**, 125 (1993).
- [34] M. A. Parkes, S. Ali, C. R. Howle, R. P. Tuckett, and A. E. R. Malins, *Mol. Phys.* **105**, 907 (2007).